The Academy of Sciences of the USSR
Scientific Centre for Biological Research
Research Computing Centre

Preprint

N.K.Balabaev, V.D.Lakhno, A.M.Molchanov (USSR)
and B.P.Atanasov (PRB)

EXTENDED ELECTRON STATES IN PROTEINS

Pushchino - 1989

The Academy of Sciences of the USSR
Scientific Centre for Biological Research
Research Computing Centre

Preprint

N.K.Balabaev, V.D.Lakhno, A.M.Molchanov (USSR)

and B.P.Atanasov (PRB)

EXTENDED ELECTRON STATES IN PROTEINS

Pushchino - 1989

A new approach to the problem of electron states in the protein molecule is described. A "dielectric cavity" model is used to study into the extended states of a protein globule which are mostly formed by the polarization field of the protein macromolecule. In a protein solution the size of such a state may be comparable with the size of the molecule. The share of the extended states in the biomolecular processes of charge transfer is discussed. Electron energies of the ground and the first excited selfconsistent states are calculated. Typical values of the predicted energies of absorption bands and luminescence are found to be ~ 1000 nm for the ground state's absorption band and ~ 2000 nm for the excited state's luminescence. Various ways of experimental observation of such states are discussed.

1. Introduction

The large-distance electron transfer is one of the central problems of molecular biology. That the electron can move to a large distance in biological systems is presently a well-established fact. Theoretical studies in this field were stimulated by de Vault and Chance /1/ who measured the temperature dependence of the rate of electron transfer from cytochrome C to chlorophyll. Currently, the predominate point of view attributes this transport to multitunnelling with unambiguously identifiable intermediate , as one of the possible mechanisms of this phenomenon /2/. The theoretical foundation of electron transfer in application to biological systems is due to Foerster/3,4/, Marcus /5/, Jortner /6/ and Hopfield /7,8/, who in turn proceeded from the idea of nonradiatory electron transfer in condensed media, which was first suggested by Peckar /9/, and Huang and Rhys /10/. The central point which allowed a deep insight into the processes of electron transfer in biological systems and which remains vital in modern exploration in the field is the representations of polaron states in condensed systems, the basic idea of the theory of nonradiatory electron transfer. (Recall that this theory started from the "polaron Hamiltonain" /9, 10/.) Therefore, research into the theory of the polaron in condensed systems may significantly broaden our knowledge of the electron states and transfer in biological systems.

The most general representation of the polaron may be given by the picture of an electron which, if placed into a polar medium, goes to a selflocalised state where it does not form chemical bonds with the atoms of the medium. This state may be imagined as an electron being trapped by a potential well formed by electron-induced polarization of the surrounding molecules of

the medium /9/. Using this representation, the authors discovered that there are multiple, not a one, discrete polaron states which have their own potential wells consistent with the electrons trapped /11, 12/. An important principal consequence is that since the first excited selfconsistent polaron state the excitation region is very large, and may include for water, ammonia and other polar liquids about $10^3 \div 10^4$ and more molecules of the medium. These findings in their turn point to the necessity of critically analyzing the problem of large-distance electron transfers, namely their biological role and impacts. This paper is just concerned with studying into these states in protein macromolecules. We shall show that the allowance for the electron large-radius states may lead to multiple new results. The very fact that they exist suggests new types of absorption and luminescence in solutions of globular proteins. For a spherically symmetric protein with electron acceptor in the centre of the globule the presence of an excited polaron state of large radius implies isotropy of binary chemical reactions under excitation.

In this paper we want to make the physical representation of the polaron in a condensed medium agree with the representation of the polaron properties of the protein molecule. We shall formulate simple mathematical models of the polaron states in the protein and discuss some of the effects which they lead to.

2. A continual model.

To introduce into what is meant by large-radius electron states in globular protein macromolecules it is necessary to examine continual representations of these objects. It is also desirable to discuss the hierarchy of continual models we will use. The representation of a protein macromolecule that takes the form of a sphere in the solution as its microphase was introduced by Bresler and Talmud /13/ who proceeded from hydrophobic properties of the protein. A progress in the modeling of protein

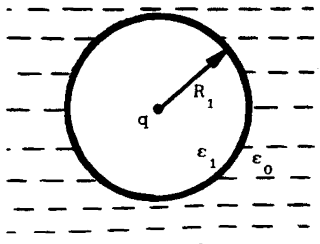

Fig. 1. A two-layer model of the protein globule.

globules led, in its turn, to a whole line of their electrostatic models /14, 15/. The simplest of them , the model of dielectric cavity, is shown in Fig.1. The model assumes that $\varepsilon_1 < \varepsilon_o$, which corresponds to a low static dielectric permittivity of the protein medium compared to the strongly polarized solvent. Stress that this model, though very simple, can give a qualitative explanation of a good many experimental findings on protein transport and electrophoresis /16/. An extension of it to a more realistic situation is shown in Fig.2. This model of a three-layer globule allows for the contribution of polar amino acid residues to dielectric permittivity in the region $R_1 < r < R_2$, for water molecules which penetrate into the superficial layer, the unsmooth surface and other factors. We assume that the solvent molecules cannot enter the region $r < R_1$. In this model $\varepsilon_1 < \varepsilon_2 < \varepsilon_0$. Physical values of dielectric permittivities can be taken from an experiment: $\varepsilon_1 \approx 4$ is the value for NN -dimetilacetamid which is the monomeric analog of protein peptide framework (the solvent impervious region $r < R_1$); $\varepsilon_0 = 80$ - is the value for water as a solvent; and the layer $R_1 < r < R_2$ is ascribed a mean value of $\varepsilon_2 \approx 40$, which in a more general sense is a parameter of the model. There are many models which assume that dielectric permittivity inside the globule depends on a coordinate (like $\varepsilon = |\vec{r}|$ /17/), and a good deal of nonlocal continual models of dielectric cavity /18/.

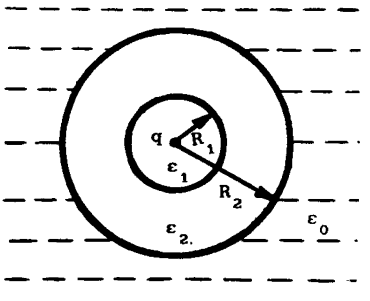

Fig. 2. A three-layer model of the protein glogule

The most important parameter for substantiating a mathematical model of polaron-type electron states in the protein globule, the parameter which justifies continual approach, is the ratio $\langle r \rangle / \bar{a}$ where $\bar{a}$ is the mean distance between two neighboring atoms of the protein molecule, and $\langle r \rangle$ is the effective polaron radius. The estimate $\bar{a}$ draws a clear distinction between a protein macromolecule and an ionic crystal for which the criterion $\langle r \rangle / \bar{a} \gg 1$ shows that the model is continual. In the ionic crystal polarization is caused by a small

deviation of ions from their equilibrium states, so that $\bar{a} \sim a$ where a is the lattice constant, and the protein molecule requires for an additional averaging if the lifetime of the electron state is much larger than the characteristic time of oscillation of twisting degrees of freedom and of deviations of macromolecular polar groups, which normally is less than 10^{-12}s. This situation is illustrated in Fig.3 which is the result of a molecular-dynamic computer simulation. In this way for the below long-living states the model of a polar medium is "more continual" in the protein molecule, than in the ionic crystal.

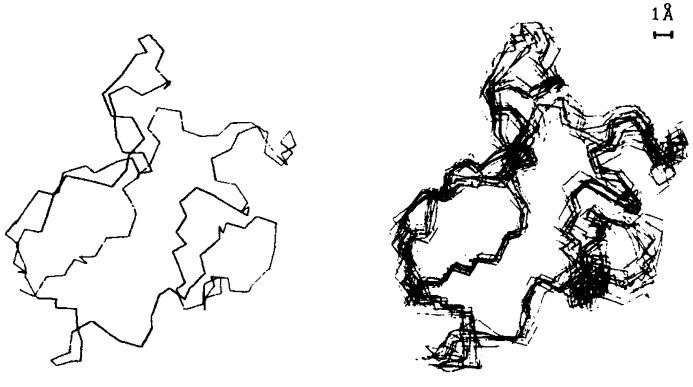

Fig.3. A plane projection of the instantaneous configuration of the main chain $(-N-C^{\alpha}-C-)_{54}$ of a ferredoxin molecule, (a), and overlapped projections for ten consecutive configurations of this molecule taken with a time Δt equal to 0.6 ps (b).

3. A polaron model for an infinite isotropic medium (according to Peckar /9/)

Polaron description of the electron state in a polar medium usually starts with the assumption that the mean Culomb field

induced by the surplus electron locally polarized the medium. Electrical field in its turn influences the electron /9/. It is essential that the electron interacts only with the inertia part of polarization it induces, so that

$$\vec{P}(\vec{r}) = \vec{P}_0(\vec{r}) - \vec{P}_\infty(\vec{r}) \qquad (1)$$

where

$$\vec{P}_0 = \frac{\varepsilon_0 - 1}{4\pi\varepsilon_0}\vec{D}\ , \qquad \vec{P}_\infty = \frac{\varepsilon_\infty - 1}{4\pi\varepsilon_\infty}\vec{D}$$

are specific dipole moments of static and high-frequency polarizations; ε_0 and ε_∞ are static and high-frequency dielectric permittivities, respectively and $\vec{D}$ is electron induction. Hence,

$$\vec{P}(r) = \frac{\vec{D}(r)}{4\pi\tilde{\varepsilon}}\ , \qquad (2)$$

$\tilde{\varepsilon}^{-1} = \varepsilon_\infty^{-1} - \varepsilon_0^{-1}$ is the effective dielectric permittivity. The vector of electric induction caused by the distributed electron charge with density $e|\Psi(\vec{r})|^2$ is equal to

$$\vec{D}(\vec{r}) = e\int |\Psi(\vec{r}')|^2 \frac{\vec{r}-\vec{r}'}{|\vec{r}-\vec{r}'|^3}\, d\vec{r}'\ , \qquad (3)$$

where $\Psi(\vec{r})$ is the wave function which can be given from the solution of the Schroedinger equation

$$\frac{\hbar^2}{2\mu}\Delta\Psi(\vec{r}) + e\Pi(\vec{r})\Psi(\vec{r}) + W\Psi(\vec{r}) = 0\ , \qquad (4)$$

where W is the electron energy. The potential $\Pi(\vec{r})$, created by the electron-induced polarization $\nabla\Pi(\vec{r}) = 4\pi\vec{P}(\vec{r})$, can, by (2) and (3), be found from the Poisson equation

$$\Delta\Pi(\vec{r}) + 4\pi\tilde{\varepsilon}^{-1}e|\Psi(\vec{r})|^2 = 0 \qquad (5)$$

The system of nonlinear differential equations (4) and (5) fully determines the state of an electron in an infinite polar medium. Peckar /9/ used variational principle to find the ground state of eqs. (4) and (5). Balabaev and Lakhno /11/ integrated

them numerically and got solutions corresponding to the excited polaron states different from the ground state. The approach we have given here will be used further to describe the polaron states in a protein globule.

4. The polaron equation for a protein globule

Our mathematical model of polaron states in the protein globule described by the model of dielectric cavity, is based on the following assumptions:

1) the globule is neutral and has zero effective surface net charge on the layer boundaries;

2) The electron states in the globule are thought of as the acceptor's potential-bound polaron states.

3) Each layer is described by a separate isotropic model of continual polar medium, and the electron wave function and the potential are assumed to be smooth both within and on the boundaries of each layer.

4) All the other assumptions are identical with those adopted to describe the polaron states in polar media /9/. For a spherically symmetric case the assumptions 1) - 4) yield the following equations for the polaron in a protein globule

$$\frac{\hbar^2}{2\mu}\left(\frac{1}{r^2}\frac{d}{dr}r^2\frac{d}{dr}\right)\Psi(r)+e(\Pi(r)+\Phi(r))\Psi(r)+W\Psi(r) = 0 \qquad (6)$$

$$\frac{1}{r^2}\frac{d}{dr}r^2\frac{d}{dr}\Pi(r) + \frac{4\pi e}{\tilde{\varepsilon}_i}\Psi^2(r) = 0 \qquad (7)$$

$$R_{i-1} < r < R_i, \quad i=1,2\ldots; \quad R_0 \equiv 0, \qquad (8)$$

where $\Phi(r)$ is the potential of acceptor

$$\Phi(r)= \begin{cases} q/\varepsilon_1 r + c_1, & r<R_1 \\ q/\varepsilon_2 r, & r>R_1 \end{cases} \qquad (9)$$

for the two-layer model of the globule ($\varepsilon_2=\varepsilon_0$) and

$$\Phi(r) = \begin{cases} q/\varepsilon_1 r + c_1', & r<R_1 \\ q/\varepsilon_2 r + c_2', & R_1<r<R_2 \\ q/\varepsilon_3 r\ , & r>R_2 \end{cases} \qquad (10)$$

for the three-layer model of the globule ($\varepsilon_3=\varepsilon_0$). $\Pi(r)$ is the potential of electron-induced polarization, μ is the electron effective mass, $\tilde{\varepsilon}_i^{-1} = \varepsilon_\infty^{-1}-\varepsilon_i^{-1}$ are the effective dielectric constants of the i-th layer, and ε_∞ is the high-frequency dielectric constant which we assume identical for all the layers.

The natural boundary solutions for eqs.(6) and (7) follow from the condition that the wave function is bounded and continual and that the potential is continual on the boundaries of globular layers, so that

$$\Psi'(0)+\frac{\mu q e}{\varepsilon_1 \hbar^2} = \Pi'(0) = 0, \quad \Psi(\infty) = \Pi(\infty) = 0$$
$$\Psi(R_i-0) = \Psi(R_i+0), \quad \Psi'(R_i-0) = \Psi'(R_i+0) \qquad (11)$$
$$\Pi(R_i-0) = \Pi(R_i+0); \ \tilde{\varepsilon}_i\Pi'(R_i-0) = \tilde{\varepsilon}_{i+1}\Pi'(R_i+0)$$

Equation (6) is the Schroedinger equation for the electron in the potential $-(\Pi+\Phi)$ which is given in a self-consistent way by (7). So, the nonlinear system of differential equations (6)-(7) with the boundary conditions (11) describes bound polaron states in the protein globule. Its solution determines the wave function of the electron state Ψ and the electron energy W , as well as the total energy of the state I_F, which is given by the functional

$$I_F[\Psi,\Pi] = \frac{\hbar^2}{2\mu}\int(\nabla\Psi)^2 d\vec{r} - e\int\Psi^2(\Pi+\Phi)d\vec{r} + \sum_i \frac{\tilde{\varepsilon}_i}{8\pi}\int_{\Omega_i}(\nabla\Pi)^2 d\vec{r} \qquad (12)$$

The last term of (12) is integrated over regions Ω_i, which correspond to the layers of the dielectric cavity model. We should stress that equations (6) and (7) may be given by an independent variation of the functional (12) with respect to the wave function $\Psi(r)$ and the potential $\Pi(r)$ with the wave function normalized by $\int\Psi^2(\vec{r})d\vec{r}=1$.

5. Solutions of polaron equations. The ground state.

The system (6)-(7) can be integrated numerically. The details of the algorithm are described in Appendix. For a homogeneous polar medium with all $\varepsilon_i = \varepsilon_0$ it yields the problem of F-centre in an ionic crystal which was solved by Lakhno and Balabaev /12/. It will be shown in Appendix that the system has a discrete set of solutions which are the selfconsistent states of electron and polarization of the globule and its surroundings. Figure 4a shows a node-free solution (zero mode), and Figure 4b the solution with a node which corresponds to the excited selfconsistent state (first mode). In this section we only dwell on the findings for the ground state.

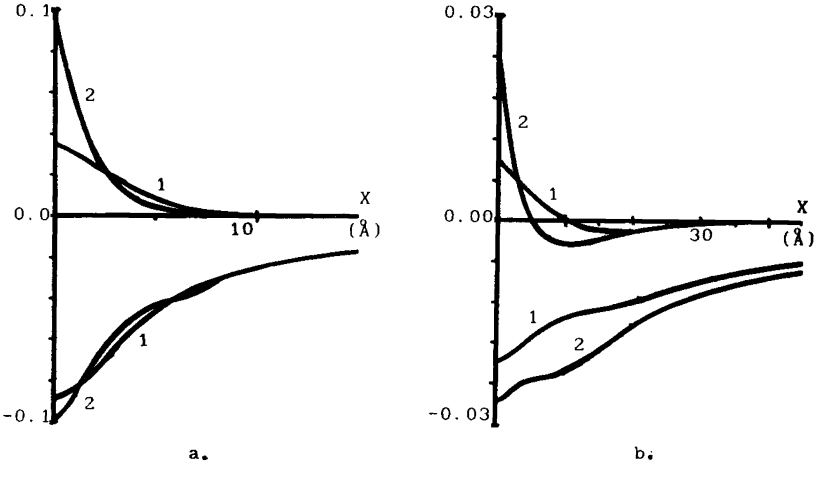

Fig.4. Solutions of the problem (6)-(7) for the two-layer (1) and the three-layer (2) models of the protein globule: a - zero mode , b - first mode. The upper part of the figure shows functions $\Psi(X)$ ($\int 4\pi X^2 \Psi^2 dX = 1$) and the lower part shows functions $\Pi(X)\,\frac{\hbar^2}{\mu e^3}$ ($\approx 0.09\,\Pi(X)$).

For tne two- and three-layer models of dielectric cavity Table 1 lists the following values which characterize the selfconsistent ground state: electron (W_{1S}) and total (I_{1S}) energies; electron levels (nonselfconsistent) in 2S (W_{2S}) and in 2P (W_{2P}) states and the corresponding total energies (I_{2S}, I_{2P}), as well as the states' radii ($\langle r\rangle_{1S}$, $\langle r\rangle_{2S}$, $\langle r\rangle_{2P}$) for both the models.

It can be seen that for the more realistic three-layer model the polaron radius in the ground state is $\langle r\rangle_{1S}$=2.3 Å, that is off the approximation of the continual model. Accordingly, the quantity $\Delta W_{1S,2P}= |W_{2P} - W_{1S}| \cong 1.2$ eV (~1000 nm) falls just into the region of transitions with charge transfers of metal-containing proteins /19/.

Table 1

Polaron states' characteristics in the protein globule

Physical value [1]	Two-layer model [2]		Three-layer model [3]	
	0-mode	1-mode	0-mode	1-mode
W_{1S}	-1.316	-0.401	-2.200	-1.035
W_{2S}	-0.529	-0.256	-0.697	-0.424
W_{2P}	-0.695	-0.283	-0.806	-0.413
I_{1S}	-0.508	-0.238	-1.243	-0.779
I_{2S}	0.280	-0.093	0.255	-0.169
I_{2P}	0.114	-0.120	0.146	-0.158
$\langle r\rangle_{1S}$	3.7	8.3	2.3	3.1
$\langle r\rangle_{2S}$	10.0	19.5	7.6	12.2
$\langle r\rangle_{2P}$	6.8	16.0	5.7	11.0

[1] The values of energies W_{1S}, W_{2S}, W_{2P} and I_{1S}, I_{2S}, I_{2P} are in eV; the avareged radii $\langle r\rangle_{1S}$, $\langle r\rangle_{2S}$, $\langle r\rangle_{2P}$ in Å.

[2] ε_1=20, ε_2=80, ε_∞=2, R_1=15Å, $\mu=m_0$, Z=1 .

[3] ε_1=4, ε_2=40, ε_3=80, ε_∞=2, R_1=7Å, R_2=15Å, $\mu=m_0$, Z=1 .

6. The excited polaron states in the protein globule

Table 1 lists besides electron (W) and total (I) energies and radii <r> in the excited selfconsistent state (2S) and the nonselfconsistent states 1S and 2P, which correspond to the potential polaron well 2S (Fig.4b). Note first of all that the radii of the excited selconsistent states of both two- and three-layer models, which are 19.5 Å and 12.2 Å, respectively, exceed largely the mean distances between neighbouring atoms $\bar{a}$ of the medium, that is continual approximation is reasonably accurate in this case. Our calculation has shown close electron energies in the selfconsistent, 2S, and nonselfconsistent, 2P, states. In the three-layer case the 2P state has a higher energy level than the 2S state. Since the dipole transfer to the 1S state is only legal from the 2P state, the excited selfconsistent 2S state can be expected to have larger lifetime in the three-layer model.

The table also yields the approximate estimate for the luminescence band for the three layer model, which is $\Delta W_{2P,1S}$ = 0.61eV (~2000 nm) i.e. lies in the far infrared range. It might be interesting to experiment with a band that, like the polaron one, could only be identified by a preliminary estimation of the qualitative effects pH, ion strength and temperature produce on the properties of the "polaron bands".

7. The dielectric cavity model and the theory of electron transfer

The above consideration evidences that the electrostatic model of the protein globule is suitable for a consistent description of various processes pertaining to photoexcitation and of electron transfer processes. For example, the probability ω that the electron of the excited selfconsistent 2S state of the protein molecule can tunnel from donor to acceptor, can be given by the following expression /6,8,20,21/:

$$\omega = L^2 \exp\left(-\frac{E_r}{\bar{\omega}}\right)(\pi/E_r T)^{1/2} \exp\left(-(E_r - J)^2/4E_r T\right) \qquad (13)$$

$$E_r = 1/8\pi\tilde{\varepsilon} \int |\vec{D}_{2S} - \vec{D}_{acs}|^2 \, d\vec{r} \,,$$

where L is the matrix element of tunnelling; $\vec{D}$ can be determined from (3), J is the reaction heat, $\bar{\omega}$ is the averaged frequency of polarization oscillations in the molecule, and E_r is the total reorganization energy of the medium. Values L and D_{acs} can only be determined if the acceptor model is defined.

It follows in particular from (3) that the tunnelling probability in the electrostatic model considered is proportional to the rate of the chemical reaction and relates to the form of the electron transfer by the tunnelling matrix element L and inductions $\vec{D}_{2S}$ and $\vec{D}_{acs}$ In this case of extended electron cases we can expect that the constant of the reaction rate should relate to pH of the solution and spatial distribution of charged aminoacid groups, since the induction $\vec{D}_{2S}[\Psi]$ of (3) depends on the polaron wave function for the most polarisable parts of the protein molecule in the layer $R_1 < r < R_2$ of our model (Fig.5).

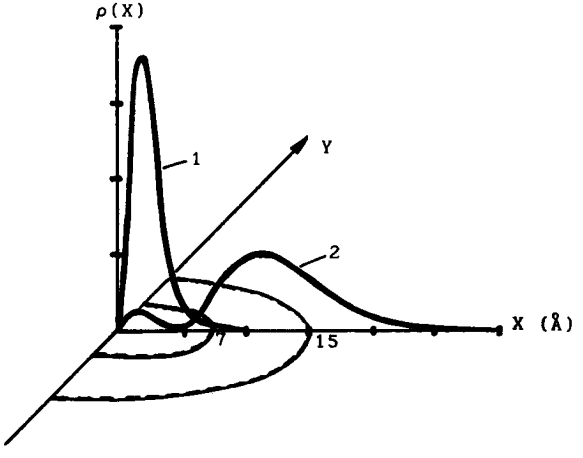

Fig. 5. Distribution of electron density in the protein globule for the three-layer model of Section 2; $\rho(X)=4\pi X^2\Psi^2(X)$; 1 is the zero mode and 2 is the first mode.

8. Discussion.

The introduced representations of large-radius extended states enable a completely new approach to the problem of electron transfer to great distances. The results of Sections 4 and 5 for the model of dielectric cavity show that the radius of the first excited state is comparable to the size of the globule, which suggests that the whole globule is involved in the process of forming such a state. If acceptor is near the globule and the extended selfconsistent state has much the same energy as one of the acceptor's electron states, then the representation of the electron as belonging to the globule or the acceptor separately makes no sense. If acceptor is far from the globule, then it is significant which is the value of the tunnelling matrix element L of the electron transfer (13). For a large-radius state it may be several orders that of a small-radius state.

Every excited self-consistent state may be ascribed configuration coordinates. For a consistent description of electron transfer it is necessary to take into account that electron can jump into intermediate selfconsistent states of acceptor and only then go to the ground state. Therefore a complex picture of electron transfer may be possible with branching the chemical reaction coordinate (see Fig. 6). This example is a very simple case where the electron from the state B to the state C may both be radiatory and non-radiatory, and in more general cases cascade radiatory and non-raditory processes are possible.

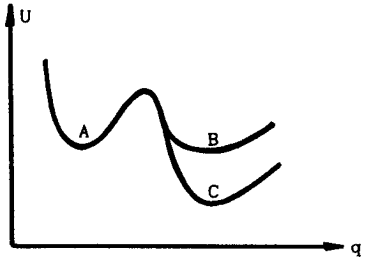

Fig. 6. Simple branching of the configuration electron transfer coordinate q.

The existence of excited selfconsistent states may lead to interesting effects on the lines of EPR and NMR, IR absorption etc, which can be used to identify these states. The discussion of these problems however is out of the scope of this paper.

Finding the polaron states in the globule

1°. We shall seek spherically symmetric solutions of differential equations (6)-(7) with boundary conditions (11) for the globule models of Figs. 1, 2. We start with passing over to new variables:

$$r = \frac{\hbar}{(2\mu|W|)^{1/2}} X , \qquad \Psi(r) = \frac{|W|}{e\hbar} \left(\frac{\mu\tilde{\varepsilon}_o}{2\pi} \right)^{1/2} Y(X) , \tag{A1}$$

$$\Pi(r) = \frac{|W|}{e} Z(X)$$

Normalization of the wave function yields:

$$|W| = \frac{2\mu e^4}{\hbar^2} \frac{1}{\tilde{\varepsilon}_0^2 \Gamma^2} , \qquad \text{where} \qquad \Gamma = \int_o^\infty Y^2(X) X^2 dX .$$

The relationships (A1) can then be rewritten as:

$$r = \frac{\hbar^2}{2\mu e^2} \tilde{\varepsilon}_0 \Gamma X , \qquad \Psi(r) = \left(\frac{2}{\pi}\right)^{1/2} \mu^{3/2} e^3 \hbar^{-3} \frac{Y(X)}{\Gamma^2 \tilde{\varepsilon}_0^{3/2}} , \tag{A1'}$$

$$\Pi(r) = \frac{2\mu e^3}{\hbar^2} \frac{Z(X)}{\Gamma^2 \tilde{\varepsilon}_0^2} .$$

We also introduce the notation $\hat{\Phi}(X)$: $\Phi(r) = \frac{|W|}{e} \hat{\Phi}(X)$.

By substituting (A1) into (6) and (7) we get equations with spherically symmetric solutions

$$\frac{d^2Y(X)}{dX^2} + \frac{2}{X} \frac{dY(X)}{dX} + Y(X)(Z(X) + \hat{\Phi}(X) - 1) = 0$$

$$\frac{d^2Z(X)}{dX^2} + \frac{2}{X} \frac{dZ(X)}{dX} + \varkappa(X) Y^2(X) = 0 . \tag{A2}$$

For the protein globule (Fig. 1)

$$\hat{\Phi}(X)=\begin{cases}\frac{N}{X}\frac{\varepsilon_0}{\varepsilon_1}+\frac{N}{X_R}\left(1-\frac{\varepsilon_0}{\varepsilon_1}\right), & X<X_R\\ \frac{N}{X_R}, & X\geq X_R,\end{cases}$$

where X_R is the scaled radius of the globule such that $R=\frac{\hbar^2}{2\mu e^2}\tilde{\varepsilon}_0\Gamma X_R$. The new parameter N is proportional to the charge q = Ze, so that

$$N=\left(\frac{2\mu}{|W|}\right)^{1/2}\frac{eq}{\hbar\varepsilon_0}=\Gamma Z\frac{\tilde{\varepsilon}_0}{\varepsilon_0}.$$

The piecewise-constant function æ(X) breaks on the surface of the globule so that

$$æ(X)=\begin{cases}\tilde{\varepsilon}_0/\tilde{\varepsilon}_1, & X<X_R\\ 1, & X\geq X_R.\end{cases}$$

Analogously, for the three-layer model of Fig.2:

$$\hat{\phi}(X)=\begin{cases}\frac{N}{X}\frac{\varepsilon_0}{\varepsilon_1}+\frac{N}{X_{R_1}}\left(\frac{\varepsilon_0}{\varepsilon_2}-\frac{\varepsilon_0}{\varepsilon_1}\right)+\frac{N}{X_{R_2}}\left(1-\frac{\varepsilon_0}{\varepsilon_2}\right), & X<X_{R_1}\\ \frac{N}{X}\frac{\varepsilon_0}{\varepsilon_2}+\frac{N}{X_{R_2}}\left(1-\frac{\varepsilon_0}{\varepsilon_2}\right), & X_{R_1}\leq X\leq X_{R_2}\\ \frac{N}{X}, & X>X_{R_2}\end{cases}$$

$$æ(X)=\begin{cases}\tilde{\varepsilon}/\tilde{\varepsilon}_1, & X<X_{R_1}\\ \tilde{\varepsilon}/\tilde{\varepsilon}_2, & X_{R_1}\leq X<X_{R_2}\\ 1, & X\geq X_{R_2}\end{cases}$$

The solutions of eqs.(A2) should satisfy the infiniteness conditions following from (11), be finite at zero and meet the corresponding internal boundary conditions at points of breaks in the piecewise-constant function æ(X).

The boundary solutions for eqs. (A2) have the form

$$2Y'(0)+N\frac{\varepsilon_0}{\varepsilon_1}Y(0)=Y(\infty)=0,\qquad Z'(0)=Z(\infty)=0 \qquad (A3)$$

For the internal boundary conditions:

$$Y(X_{R_i}-0)=Y(X_{R_i}+0), \qquad Y'(X_{R_i}-0)=Y'(X_{R_i}+0)$$
$$Z(X_{R_i}-0)=Z(X_{R_i}+0), \qquad \tilde{\varepsilon}_i Z'(X_{R_i}-0)=\tilde{\varepsilon}_{i+1} Z'(X_{R_i}+0) \qquad (A3')$$

Here i = 1 for the two-layer globule ($R_1=R$, $\tilde{\varepsilon}_2=\tilde{\varepsilon}_0$) and i = 1, 2 for the three-layer globule ($\tilde{\varepsilon}_3 \equiv \tilde{\varepsilon}_0$).

2°. The solutions of the problem (A2) with boundary conditions (A3) and internal boundary conditions (A3') were found much the same way as the solutions of the polaron problem in a homogeneous polar medium /12/. Besides, we used solutions obtained for the F-centre.

The procedure of finding solutions is quite obvious for the polaron problem in a homogeneous polar medium, therefore we shall take this case to describe the algorithm. Then, as we have already mentioned, we shall pass over to the problems which just are our immediate interest.

2.1. The equations of the polaron in a homogeneous medium can be regarded as the particular case of eqs. (A2) where $\varepsilon_i=\varepsilon_0$ and N = 0. The mathematical formulation reduces to finding the solutions of the boundary-valued problem

$$Y''(X) + \frac{2}{X} Y'(X) + Z(X)Y(X) - Y(X) = 0$$
$$Z''(X) + \frac{2}{X} Z'(X) + Y^2(X) = 0 \qquad (A4)$$
$$Y'(0)=Z'(0)=0; \qquad Y(\infty)=Z(\infty)=0$$

It was shown /11/ that this problem has a number of solutions in which $Z_n(X)$ (n=0,1,2,...) monotonically tends to zero as $X \to 0$, and $Y_n(X)$ n times crosses the axis X, after which it tends to zero as $X \to \infty$.

Now we change variables so that

$$\xi = XY, \qquad \eta = XZ$$

and equations (A4) assume the form:

$$\xi'' + \xi(\eta/X - 1) = 0$$
$$\eta'' + \xi^2/X = 0 \qquad (A5)$$

$$\xi(0)=\eta(0)=0; \qquad \xi(\infty)=\eta'(\infty)=0 \qquad (A6)$$

2.2. The solutions of (A5), which only satisfy the left-hand boundary condition of (A6) in the neighbourhood of the point $X = 0$ may be presented as power series

$$\xi(X) = a_1 X + a_2 X^2 + a_3 X^3 + \ldots$$
$$\eta(X) = b_1 X + b_2 X^2 + b_3 X^3 + \ldots$$

If we substitute these series into (A5), we can see that all coefficients a_i and b_i are expressed in terms of $a_1 \equiv a$ and $b_1 \equiv b$. Confining ourselves to several first terms of the series, we can, at a point X_0 which is not distant of $X=0$, find desiredly accurate values of $\xi(X_0; a, b)$ and $\eta(X_0; a, b)$ and their derivatives corresponding to concrete values of parameters a and b.

2.3. For the system of differential equations (A5) we define the Cauchy problem in the interval $[X_0, X_K]$. To this end, for $X = X_0$ (X_0 is small), we determine $\xi(X_0; a, b)$, $\xi'(X_0; a, b)$; and $\eta(X_0; a, b)$ and $\eta'(X_0; a, b)$ at prescribed values of a and b. Then the solution is found numerically on a computer by the standard Runge-Cutta method.

Let us notice that the second equation of (A5) yields a convex function $\eta(X)$, so that $\eta''(X)<0$ for all $X \geq 0$. This property of $\eta(X)$ is central in finding the solution of a boundary-valued problem. If we succeed in choosing the values of a and b such that $\eta(X)$ tends to a constant as $x \to \infty$, then $\xi(X)$ will tend to zero. This would mean a solution of the boundary-valued problem (A5)-(A6) is found.

2.4. Now we choose the values of parameters a and b within an interval $[X_0, X_K]$ and solve the emerging Cauchy problems. Fig.7 shows some of such solutions. Take an X_K which corresponds to the maximum of one of them, such that $a=a^*$ and $b = b^*$ (a^* and b^* - concrete numbers). Define a function to be

$$F(a, b) \equiv \eta'(X_K; a, b).$$

Let us now take the Cauchy problem for a new interval $[X_0, X_K]$, which, when solved for some a and b, will yield the values of the function $F(a, b)$. The equation

$$F(a, b) = 0 \qquad (A7)$$

is an implicit dependence between a and b. Here, the choice of X_K

determines one of the points of this dependence which is $F(a^*, b^*) = 0$.

The dependence (A7) in the prescribed intervals of a and b may be found with the CURVE program complex /22/. Figure 8 shows a curve which was obtained with this program.

The solutions of the Cauchy problem for a and b along the curve can be seen in Fig.9. An analysis of the curves $\xi(X)$ suggests the existence of a series of solutions of the boundary-valued problem (A5)-(A6). They may be arranged as follows: $\xi_n(X)$, with $n = 0,1,2,\ldots$, n times crosses the axis X, after which it exponentially tends to zero; and $\eta_n(X)$ grows monotonically to its extreme value $\eta_n(\infty)$.

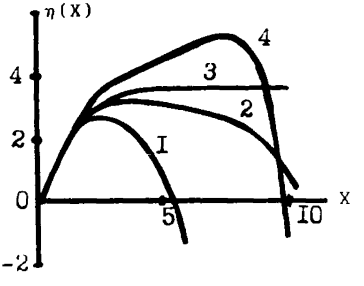

Fig.7. Functions $\eta(X)$ for various initial data given by a and b: 1 - a=1.2, b=2.0; 2 - a=1.1, b=2.0; 3 - a = 1.02, b=1.94; 4 - a=1.0, b=2.0

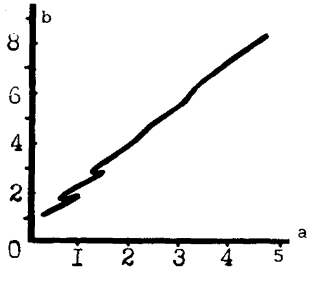

Fig. 8. Dependence between a and b following from (A6) at X = 10

2.5. Now we define a system of two functions of three variables to be

$$F_1(a,b,X_K) \equiv \xi'(X_K;a,b)$$
$$F_2(a,b,X_K) \equiv \eta'(X_K;a,b) \qquad \text{(A8)}$$

This definition means that for the values of F_1 and F_2 to be determined the Cauchy problem should be solved in the interval

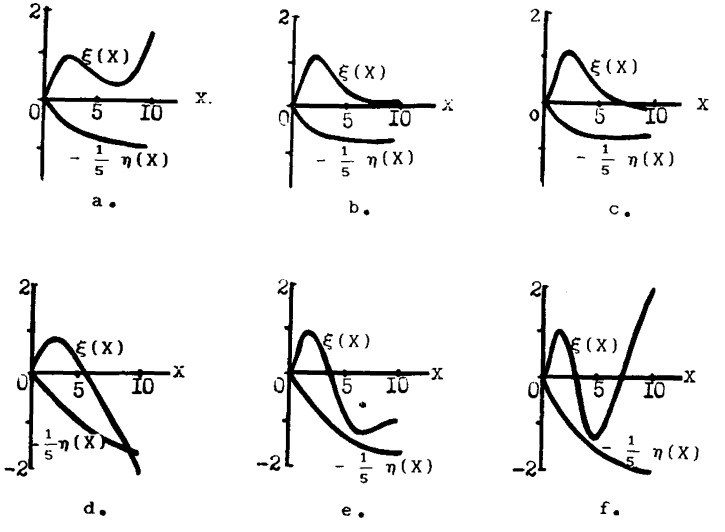

Fig.9. Solutions of the Cauchy problem for various a and b on the curve (A9) of Fig.8: a=0.733, b=1.664 (a); a=1.003, b=1.921 (b); a=1.025, b=1.942 (c); a=0.623, b=1.662 (d); a=0.900, b=2.074 (e); a=1.338, b=2.727 (f).

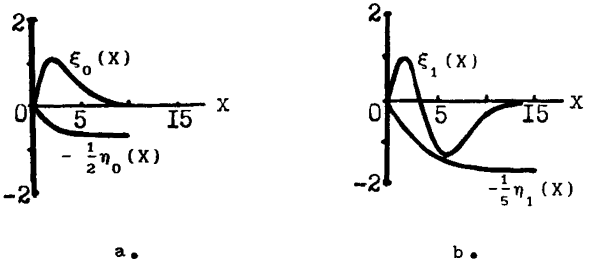

Fig.10. Solutions of the boundary-valued problem (A5)-(A6): a = 1.021, b = 1.938 (a); a = 1.091, b = 2.320 (b).

$[X_0, X_K]$ with the initial values corresponding to those of parameters a and b. The values of ξ' and η' in the end of the integration path give the values of the functions. The system of equations

$$\begin{aligned} F_1(a,b,X_K) &= 0 \\ F_2(a,b,X_K) &= 0 \end{aligned} \qquad (A9)$$

locates a curve in the space of variables a, b and X_K. We determined pieces of several branches of the curve To this end, we chose initial approximations to each branch from the calculations above, after which ran the program CURVE to find points of the curve (A9) which correspond to the values of the variables a, b, and X_K in the prescribed range.

As $X_K \to \infty$,the conditions (A9) are identical with the right-hand boundary conditions (A6). Actually, in the polaron problem we only had to go up to X_K=10 for the zero mode (n=0), X_K= 15 for the first mode (n=1) and X_K= 20 for the second mode (n=2), to get the solutions of the boundary-valued problem (A5)-(A6) accurate to several terms.

Figure 10 shows two of the solutions obtained by this procedure.

3°. The F-centre problem differs from the polaron problem for a homogeneous polar medium by additional terms NY/X in the first of equations (A3), where N is the problem's parameter. We have sought solutions for various N on the curves which pass through the polaron equations. The system of equations is

$$\begin{aligned} F_1(N,a,b) &\equiv \xi'(X_K;N,a,b) = 0 \\ F_2(N,a,b) &\equiv \eta'(X_K;N,a,b) = 0 \end{aligned} \qquad (A10)$$

The curve (A10) started from the known values at N=0 for the polaron states. The actual dependencies were found by the CURVE program. To refine the solution for a given N we introduced new functions

$$\begin{aligned} F_1(a,b,X_K) &\equiv \xi'(X_K;N,a,b) \\ F_2(a,b,X_K) &\equiv \eta'(X_K;N,a,b) \end{aligned}$$

and proceeded the way of the polaron case for system (A9).

4°. The above polaron and F-centre problems give an idea of how to find spherically symmetric polaron states in various models of the protein globule. Let us only study into the two-layer model of Fig.1, of which the case of many-layer models differs merely by technical details.

The initial model (Section 4) takes as physical parameters the values $\{\varepsilon_1, \varepsilon_2, \varepsilon_\infty, R, Z\}$. The boundary-valued problem (A2)-(A3) contains X_R and N, instead of R and Z, which are interrelated as

$$X_R = R \frac{2\mu e^2}{\tilde{\varepsilon}_0 \hbar^2} \Gamma^{-1}$$
$$N = Z \frac{\tilde{\varepsilon}_0}{\varepsilon_0} \Gamma \qquad \text{(A11)}$$

Since the value of $\Gamma = \int_0^\infty Y^2(X)X^2dX$ is not known beforehand, the values of X_R and N, which figure in the equations and correspond to preset globule radius R and charge Z, are neitherknown. What is only know is their product

$$NX_R = \frac{2\mu e^2}{\hbar^2} \frac{RZ}{\varepsilon_0} = \text{const} \qquad \text{(A12)}$$

The right-hand side of (A12) contains world constants and model parameters only. The dependence (A12) suggests the following algorithm for finding the solutions:

1-st step. We change variables as $\xi=YX$, $\eta=ZX$. Then, representing $\xi(X)$ and $\eta(X)$ as power series

$$\xi(X) = a_1X + a_2X^2 + \ldots$$
$$\eta(X) = b_1X + b_2X^2 + \ldots$$

and substituting them into (A2), we find a two-parameter family of solutions of differential equations (A2) in the neighbourhood of the point X = 0 which satisfy the left-hand boundary condition (A3). Parameters a and b are equal to $Y(0)=Y_0$ and $Z(0) = Z_0$, respectively.

2-nd step. We start from the known solutions for the F-centre. Let Y_0^*, Z_0^*, N^* be the values of medium parameters which determine a mode of the F-centre. Then, by (A12), $X_K^* = \text{const}/N^*$. The system of equations is defined to be

$$F_1(Y_0, Z_0, \varepsilon_1) \equiv \xi'(X_K; Y_0, Z_0, \varepsilon_1) = 0$$
$$F_2(Y_0, Z_0, \varepsilon_1) \equiv \eta'(X_K; Y_0, Z_0, \varepsilon_1) = 0 \qquad \text{(A13)}$$

Put $\varepsilon_1 = 80$ and $N = N^*$. Then the point $(Y_0, Z_0, \varepsilon_1) = (Y_0^*, Z_0^*, \varepsilon_0)$ will belong to the curve (A13), because of the initial values of parameters. We may make use of the CURVE program to locate the branch of the curve which passes through this point. Therefore, we can go from $\varepsilon_1 = 80$ to $\varepsilon_1 = 20$ the value which was found in the two-layer model.

3-rd step. The system of equations is

$$G_1(Y_0, Z_0, N) \equiv \xi'(X_K; Y_0, Z_0, N) = 0$$
$$G_2(Y_0, Z_0, N) \equiv \eta'(X_K; Y_0, Z_0, N) = 0 \qquad \text{(∏14)}$$

Starting from the previous solution at $\varepsilon_0 = 80$, $\varepsilon_1 = 20$ and appropriate parameter values of Y_0, Z_0, N, we locate the branch of the curve (A14) by the CURVE program. Then we calculate $\Gamma = \int_0^\infty Y^2 X^2 dX$, at each of the found points of the curve, and put

$$R = X_R \Gamma \frac{\hbar^2 \varepsilon_0}{2\mu e^2} \qquad \text{и} \qquad Z = \frac{N}{\Gamma} \frac{\tilde{\varepsilon}_0}{\varepsilon_0} .$$

We can move along the curve until we reach the parameters R = 15Å and Z = 1 (by (A12) these values will emerge at a time). In this way, we can find a solution to this case of the boundary-valued problem.

4-th step. If desired, the solution may be refined: X_K should become the parameter and should move towards larger values. Examples of solutions for the globule's polaron states are shown in Fig. 4.

5°. The spectral electron's characteristics in the potential field of selfconsistent polaron states were found by solving the linear Schroedinger equation with potential $U(X) = Z_n(X) + \hat{\Phi}(X)$, where $Z_n(X)$ is the n-th solution of the boundary-valued problem (A2)-(A3). Here however are some limitations caused by the function $Z_n(X)$ defined for a discrete sequence of ununiformly spaced points only. It is a common practice to use interpolation formulae here. But we proceeded another way. We appended the

linear Schroedinger equation

$$\zeta'' - \frac{l(l+1)}{X^2}\zeta + \zeta\left(\frac{\eta}{X} + \hat{\Phi}\right) - \lambda\zeta = 0 \qquad \text{(A15)}$$

by the following equations for polaron states

$$\begin{aligned} &\xi'' + \xi(\eta/X + \hat{\Phi}) - \xi = 0 \\ &\eta'' + \varkappa(X)\xi^2/X = 0 \end{aligned} \qquad \text{(A16)}$$

and combined the three into a one system of differential equations. The variable ζ is not included in (A16), therefore $\eta(X)$ of (A15) emerges every time in one and the same form, which also corresponds to the polaron mode at points conforming to (A15) and is independent of the values and initial data for $\zeta(X)$. At given l (orbital moment) and n (number of zero) λ was found by half-division procedure. The results are given in Table 1.

The authors are thankful to L.V. Lunevskaya and O.M. Liginchenko for their help in preparing the manuscript.

L I T E R A T U R E

1. De Vault, Chance B. Photosynthesis using a pulsed laser. 1.Temperature dependence of cytochrome oxidation rate in chromatium - Evidence for tunnelling. - Biofys.J., 1966, v.6, p.825-847.

2. Tunnelling in biological systems (Ed. Chance B.) - N.Y.; Acad.press, 1979, 386p.

3. Foerster T. - Naturwissenchaften, 1946, v.33, p.166.

4. Foerster T. - Discuss. Faraday Soc., 1959, v.27, p.7.

5. Marcus R.A. Chemical and electrochemical electron transfer theory. - Ann.Rev.Phys.Chem., 1964, v.15, p.155.

6. Jortner J. Temperature dependent activation energy for electron transfer between biological molecules. - J.Chem.Phys., 1976, v.64, No12, p.4860-4867.

7. Hopfield J.J. Electron transfer between biological molecules by thermally activated tunnelling. - Proc.Nat.Acad.Sci. USA, 1974, v.71, No9, p.3640-3644.

8. Hopfield J.J. Photo-induced charge transfer. A critical test of the mechanism and range of biological electron transfer processes. - Biophys.J., 1977, v.18, p.311-321.

9. Peckar S.I. Studies into the electron theory of crystals. - Gostekhizdat 1951.

10. Huang, K., Rhys A. -Proc.Roy.Soc, 1950 , v. 204, p 406; The theory of optical and nonradiatory transitions in the F-centre. - Problemy fiziki poluprovodnikov, IL, Moscow., 1957.

11. Balabaev N.K., Lakhno V.D. Soliton solutions in the polaron theory. -Teor. i matem. fiz., 1980, v.45, No.1, p.139.

12. Lakhno V.D. Balabaev N.K. Self-consistent states in a continual model of the F-centre and the problem of the relaxed excited state. Optika i spektroscopia, 1983, v.55, No.22, p.308.

13. Bresler S.E., Talmud D.L. On the nature of globular proteins.-Dokl.Akad.Nauk SSSR, 1944, v.43, No.7, p.326-330.

14. Tenford C., Kirkwood J.G. Theory of protein titration curves. General equations for unpenetrable spheres. - J.Am.Chem.Soc., 1957, v.79, p.5333-5339.

15. Mattew J.B. Electrostatic effects in proteins. - Ann.Rev.Biophys. Chem., 1985, v.14, p.387-417.

16. Tenford. Physical chemistry of polymers. -Chimia, Moscow, 1965.

17. Rogers K. The modelling of electrostatic interactions in the function of globular proteins. - Progress in biophysics and molecular biology, 1986, v.48, No.1, p.37-66.

18. Kornyshev A.A., Dogonadze R., Ulsirup J. - In: The Chemical Physics of Salvation, Pt.A., Amsterdam, Elsevier, 1985, p.70-116.

19. Leninger A.L. Biochemistry. The molecular basis of cell structure and function. - Worth Publishers Inc., N.-Y., 1972.

20. Zamaraev K.I., Khayrutdinov P.F., Zhdanov V.P. Tunneling of electron in chemistry. - Nauka, M., 1985.

21. Petrov E.G. Physics of electron transfer in biosystems. -Kiev, Naukova Dumka, 1984.

22. Balabaev N.K., Lunevskaya L.V. Motion along a curve in an n-dimensional space. FORTRAN Algorithms and Programs - Preprint, Pushchino, 1978.

C O N T E N T S

T13316. 9.08.89. Тираж 200 экз. Заказ 2031Р. ОНТИ
НЦБИ АН СССР в Пущине